

Four-inch high quality crack-free AlN layer grown on a high-temperature annealed AlN template by MOCVD

Shangfeng Liu^{1,2}, Ye Yuan^{2,†}, Shanshan Sheng¹, Tao Wang⁴, Jin Zhang², Lijie Huang², Xiaohu Zhang², Junjie Kang², Wei Luo², Yongde Li², Houjin Wang², Weiyun Wang², Chuan Xiao², Yaoping Liu², Qi Wang³, and Xinqiang Wang^{1,2,†}

¹State Key Laboratory of Artificial Microstructure and Mesoscopic Physics School of Physics, Nano-Optoelectronics Frontier Center of Ministry of Education, Peking University, Beijing 100871, China

²Songshan Lake Materials Laboratory, Dongguan 523808, China

³Dongguan Institute of Optoelectronics, Peking University, Dongguan 523808, China

⁴Electron Microscopy Laboratory, School of Physics, Peking University, Beijing 100871, China

Abstract: In this work, based on physical vapor deposition and high-temperature annealing (HTA), the 4-inch crack-free high-quality AlN template is initialized. Benefiting from the crystal recrystallization during the HTA process, the FWHMs of X-ray rocking curves for (002) and (102) planes are encouragingly decreased to 62 and 282 arcsec, respectively. On such an AlN template, an ultra-thin AlN with a thickness of ~700 nm grown by MOCVD shows good quality, thus avoiding the epitaxial lateral overgrowth (ELOG) process in which 3–4 μm AlN is essential to obtain the flat surface and high crystalline quality. The 4-inch scaled wafer provides an avenue to match UVC-LED with the fabrication process of traditional GaN-based blue LED, therefore significantly improving yields and decreasing cost.

Key words: AlN; high temperature annealing; MOCVD

Citation: S F Liu, Y Yuan, S S Sheng, T Wang, J Zhang, L J Huang, X H Zhang, J J Kang, W Luo, Y D Li, H J Wang, W Y Wang, C Xiao, Y P Liu, Q Wang, and X Q Wang, Four-inch high quality crack-free AlN layer grown on a high-temperature annealed AlN template by MOCVD[J]. *J. Semicond.*, 2021, 42(12), 122804. <http://doi.org/10.1088/1674-4926/42/12/122804>

1. Introduction

The explosive spread of the coronavirus disease (COVID-19) in the 2019 pandemic intensively excites the requirement for high-efficiency environmental sterilization that interrupts the most important link in the chain of disease transmission. Although plenty of conventional methods have been used, e.g. alcohol immersion, high-temperature treatment, as well as high-energy irradiation, AlGaIn-based ultraviolet-C (UVC, $\lambda \leq 280$ nm) light-emitting diode (LED) disinfection is emerging as one of the most promising and convincing avenues to confront COVID-19^[1–3]. However, when compared with conventional GaN-based blue LED, the UVC-LED only exhibits external quantum efficiency (EQE) less than 10%^[4]. One of the most crucial challenges is the difficulty of acquiring high-crystalline lattice-matched meanwhile a non-UV-absorbed substrate for upper UVC device epitaxy. Due to the short wavelength of UVC irradiation, the large band gap (>4.6 eV) is the prerequisite to screen the candidates of whom sapphire and aluminum nitride (AlN) substrates are both qualified. Unfortunately, by weighing the trade-off between large-wafer scale and lattice-match, neither of them is overall-competent: the large lattice-mismatch exhibits between sapphire and AlGaIn epilayer while the inch-scale AlN wafer prepara-

tion is still a great challenge. Direct AlN epitaxy on sapphire substrate usually accompanies high dislocation density (10^{10} cm^{-2}), which murders the device performance. Nevertheless, the proposal and verification of the face-to-face high-temperature annealing (HTA) technique obviously relieves on the above embarrassment through achieving an excellent-crystalline AlN template on sapphire substrates^[5, 6]. Subsequently, the successful regrowth of pronounced-crystalline AlN^[5, 7, 8] and AlGaIn^[9, 10] epilayers as well as a full structure UVC-LED device^[11, 12] by metal-organic chemical vapor deposition (MOCVD) unambiguously highlights the validation and prospective of such a solution.

From the viewpoint of industry and commercialization, the employment of economical AlN template, a 4-inch scaled wafer in particular would be more attractive if it exhibits the possibility to further reduce the cost of UVC-LED: (i) the cost would be intensively decreased by using crack-free 4-inch AlN template which has never been achieved to date; and (ii) the previously necessary epitaxial thickness of 3–4 μm (to acquire the qualified flat morphology and high crystalline quality for subsequent device epitaxy) would be avoided and largely save the expense of device epitaxy.

In this work, by combining the physical vapor deposition (PVD) and face-to-face HTA technique, for the first time, a 4-inch single-crystalline AlN template whose dislocation density is as low as 9.2×10^8 cm^{-2} level is achieved. On the basis of the HTA AlN template, the MOCVD regrowth of homo-epitaxial AlN layer at the 4-inch wafer scale is initialized, highlighting the prospective of wafer-sized HTA AlN templates in UVC

Correspondence to: Y Yuan, yuanye@sslabor.org.cn; X Q Wang, wangshi@pku.edu.cn

Received 28 JULY 2021; Revised 7 SEPTEMBER 2021.

©2021 Chinese Institute of Electronics

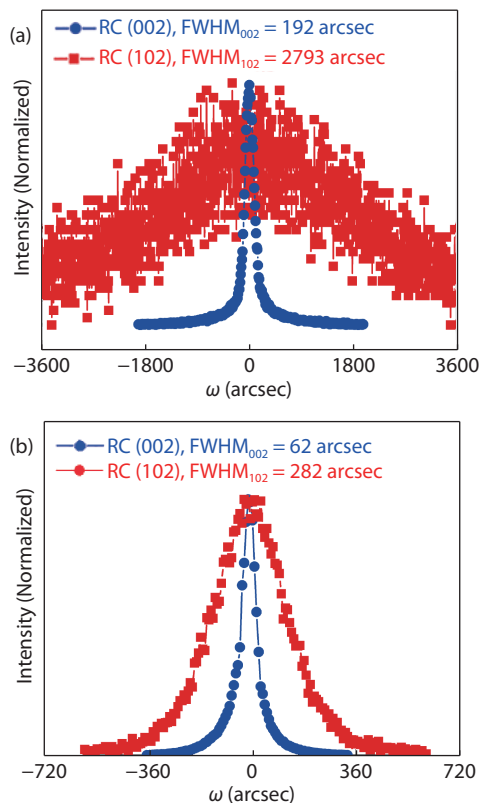


Fig. 1. (Color online) The XRD rocking curves (XRC) of (002) (circles) and (102) (squares) planes for (a) as-sputtered and (b) HTA AIN samples.

irradiation source revolution.

2. Experiment

Four-inch AlN wafers were prepared on *c*-plane sapphires by reaction magneto-sputtering technique using aluminum (purity ~ 99.999%) as the target, and the sputtering ambient was set as the mixture of argon and nitrogen as a ratio of 1 : 4. The AlN thickness was set as 500 nm by calibrating the growth speed and the sputtering power was 3000 W. Afterwards, as-sputtered AlN wafers were annealed by utilizing a tube furnace at 1700 °C for over 5 h, and the annealing ambient was nitrogen with a flow rate of 0.5 SLM. The MOCVD AlN regrowth was performed by a Prismo HiT3 MOCVD system at a temperature of 1200 °C. The regrown thickness is 200 nm. The rocking curves of AlN (002) and (102) planes were measured by X-ray diffraction (XRD, Bruker D8 Discovery) to evaluate the AlN crystallinity. High-angle annular dark-field scanning transmission electron microscopy (HAADF-STEM) was carried out in a Thermo fisher FEI Themis Z Cs probe-corrected STEM system operated at 300 kV, weak-beam dark-field (WBDF) TEM was observed using Tecnai F30 at 300 kV. The scanning electron microscopy (SEM, Hitachi Regulus 8100) and atomic force microscopy (AFM, Veeco Dimension™ 3100) with a typing mode were used to explore the surface morphology of all AlN samples.

3. Results and discussion

Fig. 1 shows XRD rocking curves (XRC) of (002) and (102) planes of as-sputtered and HTA AlN. Before the HTA treatment, the as-sputtered AlN presents *c*-oriented characteristic. The full width at half maximum (FWHM) of (002) and (102)

XRC are 192 and 2793 arcsec, respectively, which are comparable with the values of previously reported as-Al target-sputtered^[12, 13], as-AlN target-sputtered^[6, 14], as well as as-MOCVD-grown AlN films^[15]. Notably, the HTA treatment intensively improves the crystallinity of as-sputtered sample, and the FWHMs of (002) and (102) planes decrease to 62 and 282 arcsec, respectively, indicating the highly ordered re-alignment of the crystalline lattice triggered by high temperature process^[16]. According to the mosaic model, the densities of two-type dislocation are described as below^[17–19]:

$$D_{\text{dis}} = \frac{\beta^2}{4.36b^2}, \quad (1)$$

where the D_{dis} represents the density of dislocation, b is the length of Burgers vector, with values of 0.4982 and 0.3112 nm for screw- and edge-type dislocations, respectively; β represents the tilt angle β_{tilt} or twist angle β_{twist} of the mosaic structure, which are obtained by analyzing the dependence of FWHM values of XRCs on different symmetric and asymmetric planes, respectively^[17, 20–23]. It is worth noting that the HTA obviously reduces the total threading dislocation density (TDD) from 9.27×10^{10} to $9.20 \times 10^8 \text{ cm}^{-2}$, whereas the screw and edge dislocation densities decrease from 8.02×10^7 and $9.26 \times 10^{10} \text{ cm}^{-2}$ down to 8.37×10^6 and $9.19 \times 10^8 \text{ cm}^{-2}$. Such a reduction in dislocation density is mainly due to the recrystallization and lattice rearrangement process of AlN columnar crystals^[6, 24], and during which it is partially assisted by the reduction of lattice mismatch between the AlN and sapphire substrate at ultra-high temperatures. Due to the larger thermal expansion coefficient of sapphire ($\alpha_s = 8.1 \times 10^{-6} \text{ K}^{-1}$) over AlN ($\alpha_a = 4.2 \times 10^{-6} \text{ K}^{-1}$)^[25], the lattice parameters along the *a*-axis are changed from 0.3111 and 0.4758 nm to 0.3133 and 0.4824 nm for AlN and sapphire substrate from room temperature to 1700 °C, respectively, thus the lattice mismatch is reduced from 13.3% to 12.5%, which partly contributes to the improvement of excellent crystalline quality of the AlN layer.

To capture more information of the HTA AlN, the dark field cross-sectional TEM measurement was adopted, with two beam conditions carried out to analyze dislocations in different types. As shown in Figs. 2(a) and 2(b), the screw-type dislocation is nonvisible while only two edge-type dislocation lines are seen in the scanned area. Such low dislocation density agrees with XRC results. To analyze the dislocation annihilation driven by HTA operation, high-resolution HAADF-STEM was performed, focusing on the interfacial region between HTA AlN and sapphire. From the Fig. 2(c), an atomically sharp interface between sapphire and HTA AlN is visible and demonstrates a nice epitaxial nature in the high temperature treated AlN/sapphire system. However, a color-contrast region around 10 nm away from the interface is detected as a boundary between sapphire-neared N-polar AlN and upper Al-polar AlN. Actually, such a depth has been observed and verified as inversion domain boundary which consists of compound (111) γ -AlON^[13, 26, 27]. According to the Al_2O_3 -AlN-AlON system phase diagram^[26], the γ -AlON does not directly contribute to the crystalline optimization. However, as we know, the as-sputtered AlN film exhibits columnar-like AlN grains which perform lateral polarity distribution and the grain boundaries between these domains are important source of threading dislocations^[28, 29]. As shown in Fig. 2, the

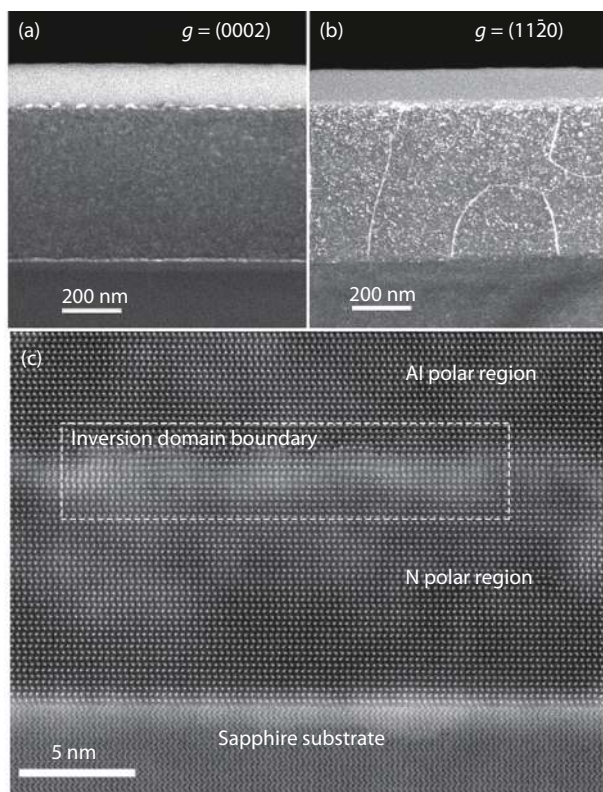


Fig. 2. Cross-sectional weak-beam dark-field (WBDF) TEM images of HTA AlN taken under diffraction conditions of (a) $g = (0002)$ and (b) $g = (11\bar{2}0)$. For $g = (0002)/(11\bar{2}0)$, the screw-type/edge-type dislocation is visible. (c) Cross-sectional high-resolution HAADF-STEM along the $[11\bar{2}0]$ direction by focusing on the interfacial region.

participation of γ -AlON successfully turns the N-polar phase into homogenous Al-polar one. Therefore, although the participation of such a γ -AlON region does not directly contribute to the crystalline improvement, it potentially suppresses the possible generation of threading dislocations from the grain boundaries between the N-polar and Al-polar regions by forming a uniform stable Al-polar epilayer.

In addition to the prospective from the application point of view, a series of fundamental experience, which possibly deepens the understand of high temperature AlN regrowth, particularly the contribution from oxides cooperation^[14], curvature^[30, 31], as well as defect evolution^[10, 32, 33], are collected. Some methods reveal new avenues to intentionally improve the high-temperature annealing film, e.g. artificially involving the domain inverse region to release the interfacial stress by fully employing oxidation^[14]. Therefore, our HTA AlN template acts as a great test bed to explore the optimization of single-crystal thin film.

The morphologies of as-sputtered, post-annealed, as well as MOCVD-regrown, AlN were studied by AFM, and the results are shown in Fig. 3. The as-sputtered AlN presents the columnar-morphology which is the same as the previously reported AlN film prepared by magneto-sputtering^[5, 6, 13], and the root mean square (RMS) is 2.62 nm. The HTA operation does not essentially change the morphology: the columnar or particle-like instead of the reported step-bunching surface with an RMS of 0.86 nm is present. Such a distinction is possibly from the different target used in the sputter process, e.g. the step-bunching morphology is mostly observed in the AlN target sputtered system^[5, 6, 9, 10, 14, 34–36], but the particle-

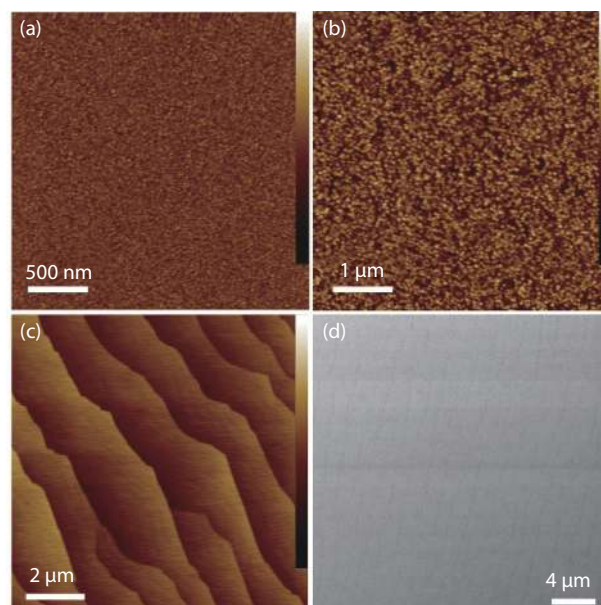


Fig. 3. (Color online) Atomic force microscopy images of (a) as-sputtered AlN, (b) HTA AlN as well as (c) MOCVD regrown AlN. (d) The SEM image of MOCVD regrown AlN on HTA AlN template. The height bar is 20 nm.

like morphology is mostly detected in the Al target sputtered one^[7], and this may affect the surficial decomposition during the annealing treatment. Nevertheless, it seems that such a rough surface does not negatively contribute to the subsequent AlN regrowth by MOCVD, and the AFM and SEM images of MOCVD-grown AlN layer are present in Figs. 3(c) and 3(d). It is seen that the as-annealed rough surface has been refreshed by the step-bunching morphology which results from the high enough diffusion length of Al atom exceeding a certain value in relation to the terrace width^[37], indicative of the ideal platform of HTA AlN for subsequent AlN-based device fabrication. The obtained morphology and RMS are both comparable with the samples prepared by epitaxial lateral overgrowth (ELOG) at high temperatures^[3]. Encouragingly, the successful epitaxy of regrown AlN fulfils the prerequisite of fabricating 4-inch UVC-LED.

When compared with a 2-inch wafer, the 4-inch AlN layer grown on sapphire by MOCVD generally exhibits larger bow and terrible cracks which is detrimental to upper epilayers and acts as the main obstacle to large-sized device epitaxy^[38, 39]. As shown in Fig. 4(b), the regrown AlN layer on 4-inch HTA template clearly shows an advantage in this viewpoint that the cracks just appear at the region around 1.5 mm away from the edge. The wafer-scaled surface cracks are visibly measured by Candela, and the results are shown in Figs. 4(c) and 4(d). It is observed that the conventional 4-inch AlN/NPSS template obtained by the ELOG process presents lots of cracks on the surface, even in the central region of the wafer. Meanwhile, as shown in Figs. 4(b) and 4(c), only a little bit roughening appears in the edge region. The comparison emphasizes the advantage of the HTA technique in achieving 4-inch-sized high-quality single-crystalline AlN template. Moreover, the FWHM values of XRC (002) and (102) planes in selected five points [shown in Fig. 4(a)] on as-annealed and post-regrown samples indicate excellent homogeneity, as shown in Table 1. In addition to crystallinity, the strain of re-

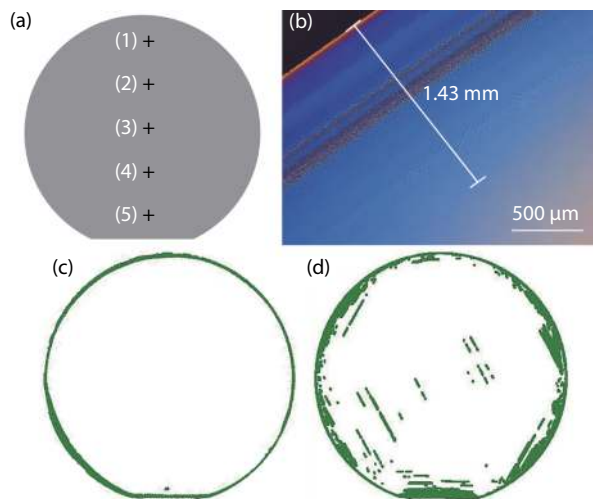


Fig. 4. (Color online) (a) Positions of five measured XRC points on 4-inch as-sputtered AlN and MOCVD regrown AlN wafers, and the results are shown in Table 1. (b) Optical microscopy image of the edge region in MOCVD regrown AlN wafer on 4-inch HTA AlN template. The images of surface cracks on (c) HTA AlN and (d) AlN/NPSS templates are measured by Candela.

Table 1. Five points XRC FWHMs and θ - ω calculated strains of 4-inch post-HTA AlN and MOCVD regrown AlN wafers.

Position	HTA AlN FWHM _{(002)/(102)} (arcsec)	Regrown AlN FWHM _{(002)/(102)} (arcsec)	Regrown AlN strain // c (%)
1	87 / 310	162 / 381	0.0869
2	64 / 288	95 / 372	0.0799
3	57 / 283	85 / 320	0.0795
4	61 / 310	78 / 312	0.0795
5	70 / 321	89 / 329	0.0807

grown AlN layer also presents a homogenous compressive feature with a value of about 0.08% as shown in Table 1.

4. Conclusion

In summary, the pronounced single-crystalline 4-inch AlN templates with dislocation density as low as $9.2 \times 10^8 \text{ cm}^{-2}$ on the *c*-plane sapphire are achieved. Thanks to such high-quality AlN template, the MOCVD regrown AlN with the thickness of only 700 nm shows comparative quality as the 3–4 μm AlN layer grown by ELOG. The exhibiting bunching-step morphology and low dislocation density in the regrown 4-inch AlN layer prove its qualification of being an ideal candidate substrate for low-cost UVC-LEDs.

Acknowledgements

This work was supported by the Key-Area Research and Development Program of Guangdong Province (Nos. 2019B121204004 and 2019B010132001), Science Challenge Project (No. TZ2018003), Basic and Application Basic Research Foundation of Guangdong Province (No. 2020A1515110891) and the National Natural Science Foundation of China (Nos. 61734001 and 61521004).

References

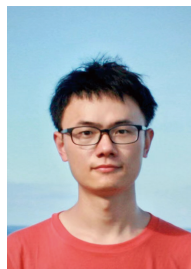
[1] Hamzavi I H, Lyons A B, Kohli I, et al. Ultraviolet germicidal irradi-

ation: Possible method for respirator disinfection to facilitate reuse during the COVID-19 pandemic. *J Am Acad Dermatol*, 2020, 82, 1511

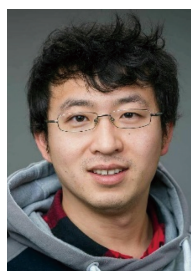
- [2] Torres A E, Lyons A B, Narla S, et al. Ultraviolet-C and other methods of decontamination of filtering facepiece N-95 respirators during the COVID-19 pandemic. *Photochem Photobiol Sci*, 2020, 19, 746
- [3] Liu S F, Luo W, Li D, et al. Sec-eliminating the SARS-CoV-2 by Al-GaN based high power deep ultraviolet light source. *Adv Funct Mater*, 2021, 31, 2008452
- [4] Kashima Y, Maeda N, Matsuura E, et al. High external quantum efficiency (10%) AlGaN-based deep-ultraviolet light-emitting diodes achieved by using highly reflective photonic crystal on p-AlGaN contact layer. *Appl Phys Express*, 2018, 11, 012101
- [5] Wang D, Uesugi K, Xiao S Y, et al. Low dislocation density AlN on sapphire prepared by double sputtering and annealing. *Appl Phys Express*, 2020, 13, 095501
- [6] Miyake H, Lin C H, Tokoro K, et al. Preparation of high-quality AlN on sapphire by high-temperature face-to-face annealing. *J Cryst Growth*, 2016, 456, 155
- [7] Huang C Y, Wu P Y, Chang K S, et al. High-quality and highly-transparent AlN template on annealed sputter-deposited AlN buffer layer for deep ultra-violet light-emitting diodes. *AIP Adv*, 2017, 7, 055110
- [8] Yoshizawa R, Miyake H, Hiramatsu K. Effect of thermal annealing on AlN films grown on sputtered AlN templates by metalorganic vapor phase epitaxy. *Jpn J Appl Phys*, 2018, 57, 01AD05
- [9] Hakamata J, Kawase Y, Dong L, et al. Growth of high-quality AlN and AlGaN films on sputtered AlN/sapphire templates via high-temperature annealing. *Phys Status Solidi B*, 2018, 255, 1700506
- [10] Uesugi K, Shojiki K, Tezen Y, et al. Suppression of dislocation-induced spiral hillocks in MOVPE-grown AlGaN on face-to-face annealed sputter-deposited AlN template. *Appl Phys Lett*, 2020, 116, 062101
- [11] Susilo N, Ziffer E, Hagedorn S, et al. Improved performance of UVC-LEDs by combination of high-temperature annealing and epitaxially laterally overgrown AlN/sapphire. *Photon Res*, 2020, 8, 589
- [12] Susilo N, Hagedorn S, Jaeger D, et al. AlGaN-based deep UV LEDs grown on sputtered and high temperature annealed AlN/sapphire. *Appl Phys Lett*, 2018, 112, 041110
- [13] Hagedorn S, Walde S, Mogilatenko A, et al. Stabilization of sputtered AlN/sapphire templates during high temperature annealing. *J Cryst Growth*, 2019, 512, 142
- [14] Xiao S Y, Suzuki R, Miyake H, et al. Improvement mechanism of sputtered AlN films by high-temperature annealing. *J Cryst Growth*, 2018, 502, 41
- [15] Wang M X, Xu F J, Xie N, et al. High-temperature annealing induced evolution of strain in AlN epitaxial films grown on sapphire substrates. *Appl Phys Lett*, 2019, 114, 112105
- [16] Gu W, Liu Z B, Guo Y N, et al. Comprehensive study of crystalline AlN/sapphire templates after high-temperature annealing with various sputtering conditions. *J Semicond*, 2020, 41, 122802
- [17] Metzger T, Höppler R, Born E, et al. Defect structure of epitaxial GaN films determined by transmission electron microscopy and triple-axis X-ray diffractometry. *Philos Mag A*, 1998, 77, 1013
- [18] Pantha B N, Dahal R, Nakarmi M L, et al. Correlation between optoelectronic and structural properties and epilayer thickness of AlN. *Appl Phys Lett*, 2007, 90, 241101
- [19] Ayers J E. The measurement of threading dislocation densities in semiconductor crystals by X-ray diffraction. *J Cryst Growth*, 1994, 135, 71
- [20] Srikant V, Speck J S, Clarke D R. Mosaic structure in epitaxial thin films having large lattice mismatch. *J Appl Phys*, 1997, 82, 4286
- [21] Chierchia R, Böttcher T, Heinke H, et al. Microstructure of heteroepitaxial GaN revealed by X-ray diffraction. *J Appl Phys*, 2003, 93,

8918

- [22] Heinke H, Kirchner V, Einfeldt S, et al. X-ray diffraction analysis of the defect structure in epitaxial GaN. *Appl Phys Lett*, 2000, 77, 2145
- [23] Wang X Q, Che S B, Ishitani Y, et al. Threading dislocations in In-polar InN films and their effects on surface morphology and electrical properties. *Appl Phys Lett*, 2007, 90, 151901
- [24] Hagedorn S, Walde S, Knauer A, et al. Status and prospects of AlN templates on sapphire for ultraviolet light-emitting diodes. *Phys Status Solidi A*, 2020, 217, 1901022
- [25] Yim W M, Paff R J. Thermal expansion of AlN, sapphire, and silicon. *J Appl Phys*, 1974, 45, 1456
- [26] Fukuyama H, Miyake H, Nishio G, et al. Impact of high-temperature annealing of AlN layer on sapphire and its thermodynamic principle. *Jpn J Appl Phys*, 2016, 55, 05FL02
- [27] Akiyama T, Uchino M, Nakamura K, et al. Structural analysis of polarity inversion boundary in sputtered AlN films annealed under high temperatures. *Jpn J Appl Phys*, 2019, 58, SCCB30
- [28] Kamohara T, Akiyama M, Ueno N, et al. Influence of sputtering pressure on polarity distribution of aluminum nitride thin films. *Appl Phys Lett*, 2006, 89, 243507
- [29] Kaur J, Kuwano N, Jamaludin K R, et al. Electron microscopy analysis of microstructure of postannealed aluminum nitride template. *Appl Phys Express*, 2016, 9, 065502
- [30] Yoshikawa A, Nagatomi T, Morishita T, et al. High-quality AlN film grown on a nanosized concave-convex surface sapphire substrate by metalorganic vapor phase epitaxy. *Appl Phys Lett*, 2017, 111, 162102
- [31] Hayashi Y, Tanigawa K, Uesugi K, et al. Curvature-controllable and crack-free AlN/sapphire templates fabricated by sputtering and high-temperature annealing. *J Cryst Growth*, 2019, 512, 131
- [32] Ben J W, Sun X J, Jia Y P, et al. Defect evolution in AlN templates on PVD-AlN/sapphire substrates by thermal annealing. *CrystEngComm*, 2018, 20, 4623
- [33] Uedono A, Shojiki K, Uesugi K, et al. Annealing behaviors of vacancy-type defects in AlN deposited by radio-frequency sputtering and metalorganic vapor phase epitaxy studied using monoenergetic positron beams. *J Appl Phys*, 2020, 128, 085704
- [34] Uesugi K, Hayashi Y, Shojiki K, et al. Reduction of threading dislocation density and suppression of cracking in sputter-deposited AlN templates annealed at high temperatures. *Appl Phys Express*, 2019, 12, 065501
- [35] Uesugi K, Hayashi Y, Shojiki K, et al. Fabrication of AlN templates on SiC substrates by sputtering-deposition and high-temperature annealing. *J Cryst Growth*, 2019, 510, 13
- [36] Shojiki K, Uesugi K, Kuboya S, et al. High-quality AlN template prepared by face-to-face annealing of sputtered AlN on sapphire. *Phys Status Solidi B*, 2021, 258, 2000352
- [37] Bryan I, Bryan Z, Mita S, et al. Surface kinetics in AlN growth: A universal model for the control of surface morphology in III-nitrides. *J Cryst Growth*, 2016, 438, 81
- [38] Okada N, Kato N, Sato S, et al. Growth of high-quality and crack free AlN layers on sapphire substrate by multi-growth mode modification. *J Cryst Growth*, 2007, 298, 349
- [39] Banal R G, Akashi Y, Matsuda K, et al. Crack-free thick AlN films obtained by NH₃Nitridation of sapphire substrates. *Jpn J Appl Phys*, 2013, 52, 08JB21



Shangfeng Liu got his BS degree from Sichuan University in 2017. Now he is a PhD student at the School of Physics, Peking University, under the supervision of Prof. Xinqiang Wang. His research focuses on material epitaxy of nitride material by MOCVD and physics of optoelectronic devices.



Ye Yuan got his BS and MS degrees from the Harbin Institute of Technology in 2011 and 2013, respectively. Afterwards, he got a PhD from Technische Universität Dresden in 2017. Then he joined Helmholtz-Zentrum Dresden-Rossendorf and King Abdullah University of Science and Technology as postdoc in 2017 and 2018, respectively. In 2019, he joined Songshan Lake Materials Laboratory as an associate investigator. His research mainly focuses on the growth and physics in wide bandgap semiconductors, as well as the application of ion beam in semiconductors.



Xinqiang Wang is a full Professor of School of Physics at Peking University. He joined the faculty on May 2008, after more than 6 years' postdoctoral research at Chiba University and Japan Science Technology Agency, Japan. He has received the China National Funds for Distinguished Young Scientists in 2012 and has been awarded Changjiang Distinguished Professor by Ministry of Education in 2014. He mainly concentrates on III-nitrides compound semiconductors including epitaxy and device fabrication. He is the author or co-author of 200+ refereed journal articles with over 3800 citations and has delivered over 40 invited talks at scientific conferences and contributed three chapters in three books.